Soft Matter

PAPER

View Article Online
View Journal | View Issue

Cite this: *Soft Matter*, 2022, **18**, 2149

Multi-level encryption of information in morphing hydrogels with patterned fluorescence†

Li Xin Hou,‡ Hongyao Ding,‡ Xing Peng Hao, Chao Nan Zhu, Miao Du, Zi Liang Wu* and Qiang Zheng*

Fluorescent hydrogels have attracted tremendous attention recently in the field of information security due to the booming development of information technology. Along this line, it is highly desired to improve the security level of concealed information by the advancements of materials and encryption technologies. Here we report multi-level encryption of information in a bilayer hydrogel with shape-morphing ability and patterned fluorescence. This hydrogel is composed of a fluorescence layer containing chromophore units in the poly(acrylic acid) network and an active layer with UV-absorption agents in the poly(*N*-isopropylacrylamide-*co*-acrylic acid) network. The former layer exhibits tunable fluorescence tailored by UV light irradiation to induce unimer-to-dimer transformation of the chromophores, facilitating the write-in of information through photolithography. The latter layer is responsive to temperature, enabling morphing of the bilayer hydrogel. Therefore, the bilayer hydrogel encoded with patterned fluorescent patterns can deform into three-dimensional configurations at room temperature to conceal the information, which is readable only after successive procedures of shape recovery at an appropriate temperature and under UV light irradiation from the right direction. The combination of morphing materials and patterned fluorescence as a new avenue to improve the encryption level of information should merit the design of other smart materials with integrated functions for specific applications.

Received 17th January 2022,
Accepted 12th February 2022

DOI: 10.1039/d2sm00083k

rsc.li/soft-matter-journal

Introduction

With the rapid development of information technology, information security has become a significant concern in daily life, especially in the fields of economy and military. So far, many strategies have been employed for data encryption, such as holographic imaging,[1,2] photonic crystals,[3,4] watermarks,[5,6] and patterned fluorescence/phosphorescence.[7–13] Among these methods, fluorescence imaging has aroused tremendous attention as it becomes readable only under ultraviolet light irradiation with an appropriate wavelength, rather than in daylight.[14,15] Owing to their close similarity to soft biotissues and promising applications in aqueous and biological environments,[16–19] hydrogels are recognized as ideal materials to carry fluorescent information.[8,20–22] For example, Ji *et al.* prepared a set of fluorescent supramolecular hydrogels containing different chromophores.[23] The obtained hydrogels were assembled into different code arrays to deliver fluorescent information. However, the information encrypted in the planar sheet could be easily detected in the presence of ultraviolet (UV) light. It is highly desired to improve information security by multi-level encryption of the information.

Many hydrogels are responsive to external stimuli,[24–26] which are widely used to devise morphing structures[27–30] and in soft actuators[31–35] and soft robots.[36–39] Such shape-changing ability of hydrogels has been harnessed to enhance information security in recent years, which can upgrade the encryption level of information in terms of morphing structures.[13,40] The encrypted message is not accessed directly in a simple way, but revealed after the shape recovery as a necessary decryption process. For example, dual-encryption of information was achieved in a hydrogel by shape changing and site-specific quenching of the fluorescence by wet-stamping and diffusion of metallic ions. Both the shape change and patterned fluorescence are based on the local chemical changes in the hydrogel. The molecular diffusion and physical interaction might lead to poor stability of the fluorescent information and irreversible deformation of the gel.[41] However, most of the single-layer morphing hydrogels are somewhat transparent and partial information can be detected under UV light, which leads to

Ministry of Education Key Laboratory of Macromolecular Synthesis and Functionalization, Department of Polymer Science and Engineering, Zhejiang University, Hangzhou 310027, China. E-mail: wuziliang@zju.edu.cn, zhengqiang@zju.edu.cn

† Electronic supplementary information (ESI) available: Additional information on tensile stress–strain curves, fluorescence spectra, swelling behaviors of the hydrogels (PDF). See DOI: 10.1039/d2sm00083k

‡ They contributed equally to this work.

information leakage. We envision to improve the performance and encryption level of information in a bilayer hydrogel by orthogonally creating a stable patterned fluorescence and gradient structure for reversible shape change.

In this paper, we demonstrate multi-level encryption of information in a bilayer hydrogel capable of shape morphing to conceal the fluorescent information at room temperature, which become readable at elevated temperatures and under UV light. The bilayer gel consists of a thermo-responsive hydrogel as the active layer and another passive hydrogel layer containing chemically grafted chromophores, 4′-(*N*-vinyl benzyl-4-pyridinyl)-2,2′,6′,2″-terpyridine perchlorate (VPTP).[40,42] The fluorescence of the passive layer can be facilely tuned by UV light irradiation to induce unimer-to-dimer transformation of the chromophores,[43,44] which facilitates the write-in of fluorescent information by photolithography. To further avoid the information leakage at room temperature, UV-absorbing agents are incorporated into the outer active layer to prevent the penetration of UV light to the inner passive layer to light on the fluorescent information. Therefore, the encrypted information in the deformed hydrogel is well protected at room temperature even under UV light. To decrypt the concealed information, the deformed bilayer hydrogel needs to be placed in hot water to trigger the shape recovery to flat, and then under UV light irradiation from the side of the passive layer to reveal the fluorescent information. This work provides a new design for improved information security and enhanced stability of the information in hydrogels, which should broaden the application of gel materials in information storage and display.

Experimental section

Materials

Acrylic acid (AAc), *N*-isopropylacrylamide (NIPAAm), *N*,*N*′-methylenebis(acrylamide) (MBAA, the chemical crosslinker), and potassium persulfate (KPS, the initiator) were received from Aladdin Chemistry Co., Ltd. The fluorescent monomer, 4′-(*N*-vinyl benzyl-4-pyridinyl)-2,2′,6′,2″-terpyridine perchlorate (VPTP), was synthesized according to the protocol reported in the literature.[40,42] Bumetrizole (UV-326, the UV-absorbing agent) was purchased from Shanghai D&B Chemical Technology Co., Ltd. Dimethyl sulfoxide (DMSO) was bought from Sinopharm Chemical Reagent Co., Ltd. Deionized water was used in all the experiments.

Preparation of the bilayer hydrogel

The bilayer hydrogel was prepared by two-step polymerization. The poly(AAc-*co*-VPTP) gel was fabricated first. AAc (3 mol L^{-1}), VPTP (5 mg mL^{-1}), KPS (0.5 mol%, relative to the total monomers), and MBAA (3 mol%, relative to the total monomers) were dissolved in DMSO to form a homogeneous precursor solution, which was injected into a reaction cell consisting of two glass substrates separated by a silicone rubber spacer with a 0.5 mm thickness. Subsequently, the reaction cell was kept in an oven at 60 °C for 6 hours. When the polymerization was completed, the silicone rubber spacer of the reaction cell was changed to a thicker one (thickness of 1 mm) for the fabrication of the second hydrogel layer of poly(AAc-*co*-NIPAAm). Another precursor solution containing NIPAAm (2.7 mol L^{-1}), AAc

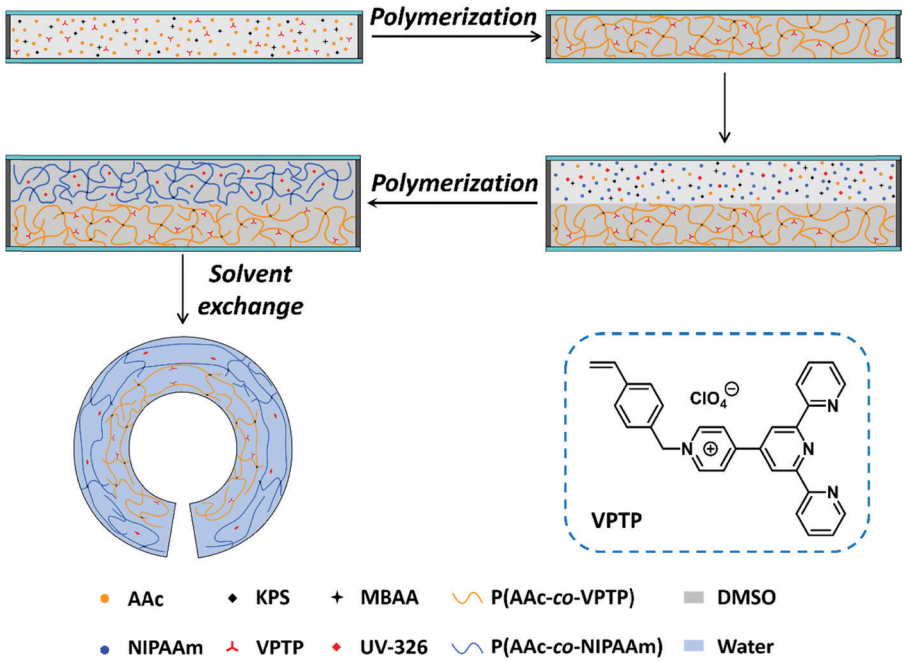

Fig. 1 Schematic illustration of the procedure for preparing the bilayer hydrogel by two-step polymerization and subsequent solvent exchange from DMSO to water.

(0.3 mol L^{-1}), KPS (0.5 mol%), MBAA (3 mol%), and UV-326 (5 mg mL^{-1}) with DMSO as the solvent was injected into the extra space of the same reaction cell, which was placed in the oven at 60 °C for another 6 hours to complete the polymerization and form the bilayer organogel. The resultant bilayer organogel was immersed in a large amount of water for solvent exchange for one week to remove the residuals and thus the equilibrated bilayer hydrogel was obtained. The poly(AAc-*co*-VPTP) and the poly(AAc-*co*-NIPAAm) hydrogels are abbreviated as PAV and PAN gels and named the passive and active layers, respectively, according to their distinct responses to external stimuli. Other single-layer PAV and PAN gels were prepared in a similar way.

Characterization

The mechanical properties of the hydrogels were measured by using a commercial tensile tester (Instron 3343). Dumbbell-shaped samples were cut from the hydrogel sheets with an initial gauge length of 12 mm and a width of 2 mm. The tensile tests were performed at room temperature with a stretch rate of 100 mm min^{-1}. The stress–strain curves were recorded, and the Young's modulus of the hydrogel was calculated from the initial slope of the stress–strain curve with a strain below 10%. At least three parallel tests were performed for each hydrogel. The UV-vis spectra of the PAN hydrogels with or without UV-326 over the wavelength range of 200–800 nm were measured using a UV-1800 spectrophotometer (Shimadzu). The fluorescence spectra of the PAV hydrogel were obtained at room temperature by using an RF-6000 fluorescence spectrometer (Shimadzu). The swelling ratio in length of the gel, S, was calculated by $S = L_1/L_0$, in which L_1 and L_0 are the diameter of the hydrogel disk equilibrated in water at a certain temperature and the diameter of the as-prepared organogel disk, respectively. The curvature of the bilayer hydrogel, k, at a certain temperature was calculated by $k = 1/R$, where R is the radius of the hydrogel arch.

Results and discussion

The bilayer hydrogel, consisting of the poly(AAc-*co*-NIPAAm) (PAN) gel as the active layer and the poly(AAc-*co*-VPTP) (PAV) gel as the passive layer, was fabricated by two-step polymerization, as illustrated in Fig. 1. UV-326 was added to the active layer to prevent the UV light penetration to the passive layer when irradiated from the side of the active layer. We should note that the bilayer gel was developed by using DMSO as the solvent by considering the solubility of VPTP and UV-326. The bilayer hydrogel was obtained after swelling the organogel in water for solvent exchange at room temperature, accompanied by bending of the gel to form a roll due to the swelling mismatch between the active and passive layers. To enable the encryption of fluorescent information in the deformed bilayer gel, the active layer should have a relatively large swelling ratio so that it will be outside of the roll. To optimize the deformation of the bilayer hydrogel, the swelling ratio in length, S, of PAV and PAN hydrogels at room temperature (~25 °C) was tuned by the

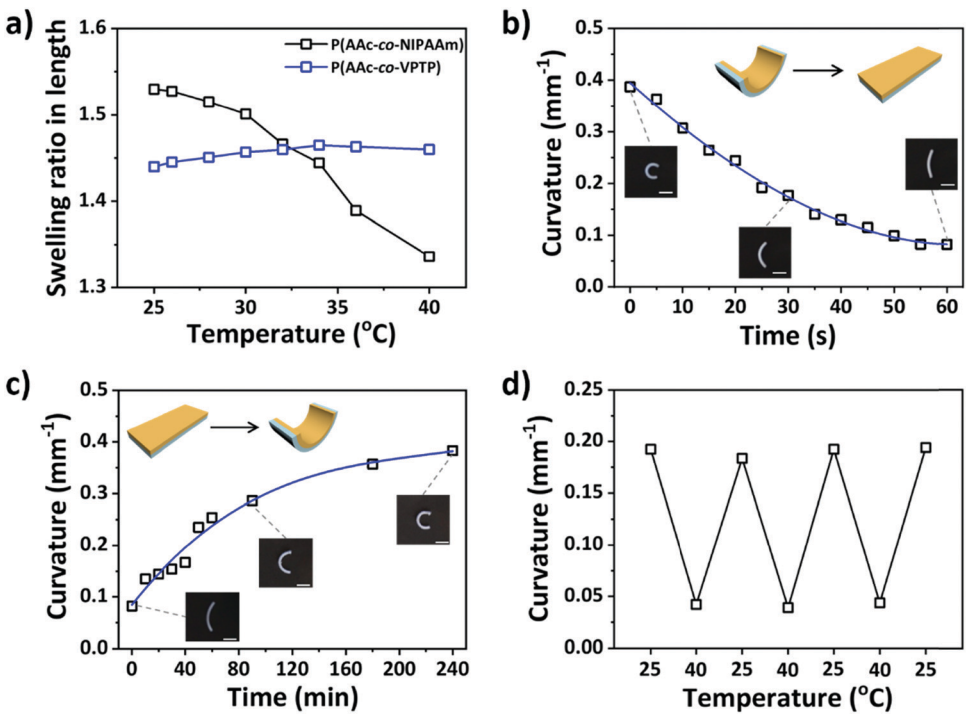

Fig. 2 Thermo-response of the single-layer hydrogel and deformation of the bilayer hydrogel. (a) Swelling ratio in length of PAN and PAV hydrogels at different temperatures. (b and c) Variation of the curvature of the bilayer hydrogel during the deformation process after being transferred from a 25 °C to a 40 °C water bath (b) and then being transferred back to the 25 °C water bath (c). Inset photos show the shapes of the bilayer gel during the deformation process. Scale bar, 1 cm. (d) Curvature change of the bilayer hydrogel during cyclic heating–cooling processes.

feeding concentration of the chemical crosslinker. As expected, the S values of both PAV and PAN gels decrease with an increase in the concentration of the crosslinker (Fig. S1, ESI†). When the crosslinker concentration of both gels was 3 mol% (relative to the total monomers), the S value of the PAV gel was smaller than that of the PAN gel, which was a prerequisite for bending deformation of the bilayer gel to hide the PAV layer inside the roll. In addition, the PAV and PAN gels had similar Young's modulus values of 71.9 kPa and 89.8 kPa, respectively (Fig. S2, ESI†). Therefore, the crosslinker concentration was kept at 3 mol% for the preparation of the bilayer gel.

The reversible shape change of the bilayer hydrogel is closely related to the variation of swelling mismatch between the active and passive layers under different conditions. Therefore, we investigated the dimension change of single PAV and PAN hydrogels and the deformation of the bilayer hydrogel at different temperatures (Fig. 2). We should note that the swelling ratio in length, S, of the single layer hydrogels was calculated with the as-prepared organogels as the reference. As shown in Fig. 2a, the S value of the PAN gel decreased from 1.53 to 1.33 as the temperature increased from 25 °C to 40 °C because of the thermo-responsiveness of PNIPAAm segments. In contrast, the S value of the PAN gel maintained a constant value of ~1.45 due to the nonresponsive nature of the copolymer. The variation of the differential swelling ratio between the two gels with temperature was beneficial to the dynamic adjustment of the swelling mismatch and thus the reversible deformation of the bilayer gel. We also examined the dimension change of PAV and PAN gels with time after switching the incubation bath from 25 °C to 35, 40, or 50 °C (Fig. S3, ESI†). The PAV gel showed small changes in dimensions at elevated temperatures, while the PAN gel contracted with time and reached the equilibrium state after several minutes at elevated temperatures. The different thermo-responses of PAV and PAN gels lay the foundation for controllable deformation of the bilayer gel which will be described as follows.

As expected, the bilayer hydrogel formed a roll at room temperature due to the swelling mismatch between the two layers. The deformations of the bilayer gel after switching the incubation conditions between 25 °C and 40 °C were investigated. As shown in Fig. 2b, when being transferred from the 25 °C to 40 °C water bath, the bilayer gel recovered its shape from the roll to flat in 60 seconds, accompanied by a decrease in the curvature of the gel from 0.4 to 0.1 mm^{-1}. Regarding the time difference to reach the equilibrium state between the singular PAN gel and the bilayer gel (Fig. 2b and Fig. S3b, ESI†), it should be associated with the different contents of the PAN matrix. As the bilayer gel was prepared by two-step polymerization, part of the NIPAAm monomer permeated into the preformed PAV layer, resulting in a relatively low content of the copolymer in the PAN layer compared to that in the control system of the singular PAN gel. The relatively low content of

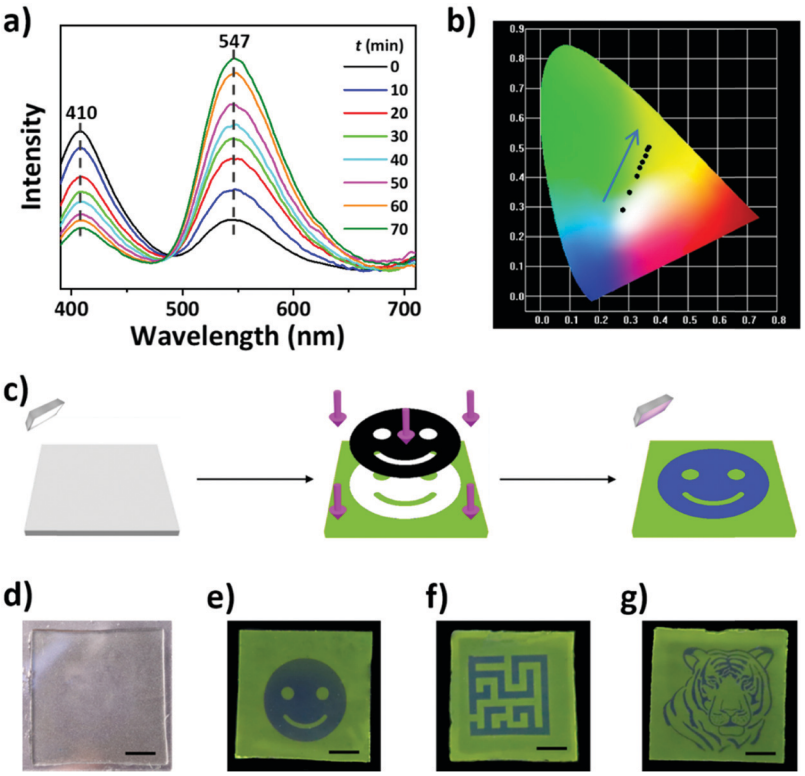

Fig. 3 Tunable fluorescence behavior of the PAV hydrogel. (a and b) Fluorescence spectra (a) and the corresponding CIE chromaticity diagram (b) of the PAV gel under 365 nm UV light irradiation for different periods of time. The feeding concentration of VPTP was 1 mg mL^{-1}. (c) Schematic illustration of the creation of fluorescent patterns in the PAV gel by photolithography. The light-exposed regions and unexposed regions showed yellow-green and blue fluorescence, respectively. (d–g) Digital photos of the patterned PAV gels in daylight (d) and under UV light (e–g). Scale bar, 1 cm.

PAN should be responsible for the faster response speed of the bilayer hydrogel and shorter time to reach the equilibrium state. After switching back the incubation conditions from 40 °C to 25 °C, the bilayer gel gradually bent to the roll configuration in 240 minutes (Fig. 2c). The relatively low bending speed, compared to the shape recovery process, was related to the asymmetry changing speed of the conformation of PNIPAAm segments during the heating and cooling processes. The inset photos in Fig. 2b and c show that the ultimate shape of the bilayer hydrogel after the heating and cooling processes was almost the same as the initial one, which promised the repeatable deformation of the bilayer gel mediated by the change of temperature. The reversible deformation was examined by measuring the curvature of the bilayer gel during cyclic incubation of the gel at 25 °C and 40 °C; the result shown in Fig. 2d indicated the good reversibility of the bending deformation of the bilayer gel, which is important for the information encryption that will be demonstrated in the following.

Besides shape morphing, another design for encryption of information in the bilayer hydrogel is to create patterned fluorescence that is not readable in daylight and only becomes readable under UV light. The PAV hydrogel containing the chromophores of VPTP showed tunable fluorescence mediated by UV light irradiation to induce the unimer-to-dimer transformation of the chromophores.[40,42] Under the acidic conditions of the PAV gel containing AAc groups, the side peripheral pyridyl group of the chromophores becomes protonated, resulting in more planar conformation. Density functional theory calculations indicated that the dimer had a smaller Gibbs free energy than the unimer. Therefore, additional light irradiation facilitated the unimer-to-dimer transformation by providing external energy to overcome the energy barrier.[40] Fig. 3a shows the fluorescence spectra of the PAV gel after being irradiated with 365 nm UV light for different periods of time; the spectra generally included a large blue emission peak at ~410 nm and a small yellow emission peak at ~547 nm with different relative intensities. Before the photo-treatment, the PAV gel exhibited blue fluorescence emission, suggesting that most chromophores in the gel matrix were in the unimer state.[42] As the time of UV light irradiation increased, the chromophores changed their state from unimer to dimer, resulting in a decreased intensity of the blue emission and an increased intensity of yellow emission.[43–45] As shown in the CIE chromaticity diagram (Fig. 3b), the fluorescence color of the PAV gel varied from light blue to yellow-green, corresponding to the variation of coordinate values from (0.275, 0.291) to (0.363, 0.503). We also examined the influence of the feeding concentration of VPTP on the fluorescence properties of the PAV gel; the fluorescence spectra and CIE chromaticity diagram (Fig. S4, ESI†) showed similar tunable fluorescence. Such tunable fluorescence is utilized to create patterned information that is concealed in daylight.[46–48]

Patterned information was encoded in the PAV layer by means of photolithography under UV light to locally tune the fluorescence behavior (Fig. 3c). The unexposed regions retained

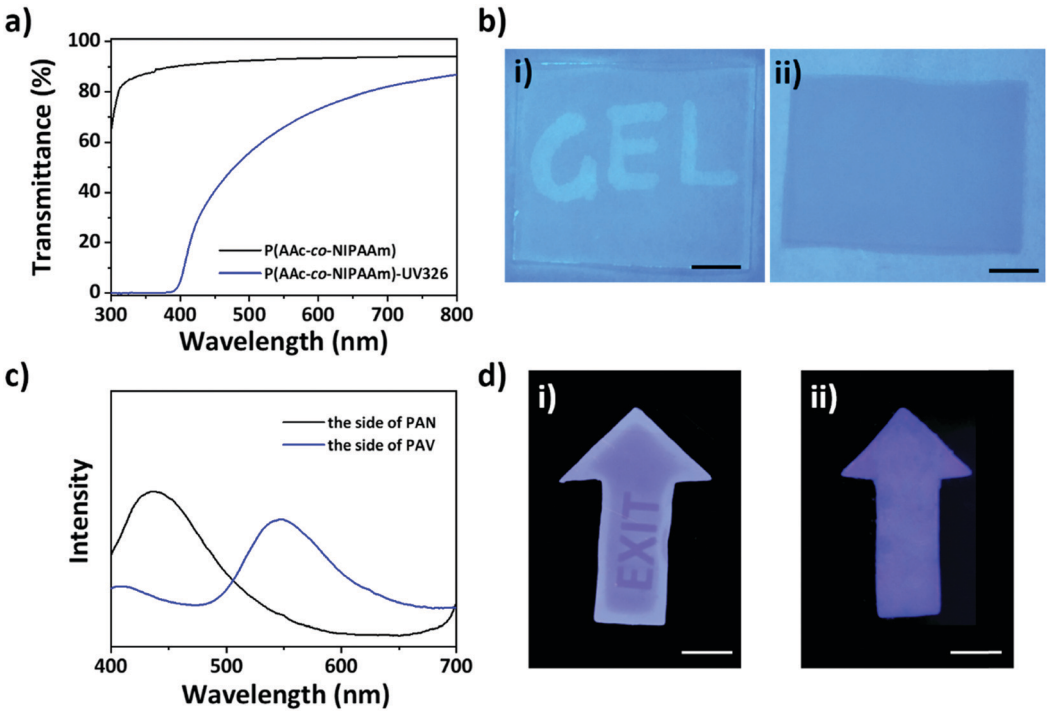

Fig. 4 Information protection in the hydrogel by incorporating UV-absorbing agents. (a) UV-visible spectra of the PAN gels with and without UV-326. (b) Photos of the gels without (i) and with (ii) UV-326 placed atop a paper with characters written using fluorescein sodium under 365 nm UV light. (c) Fluorescence spectra of the bilayer gel after UV light irradiation from the side of the PAN layer and PAV layer. Excitation wavelength: 365 nm. (d) Photos of the bilayer gel under 365 nm UV light from the side of the PAV layer (i) and the side of the PAN layer. Scale bar, 5 mm.

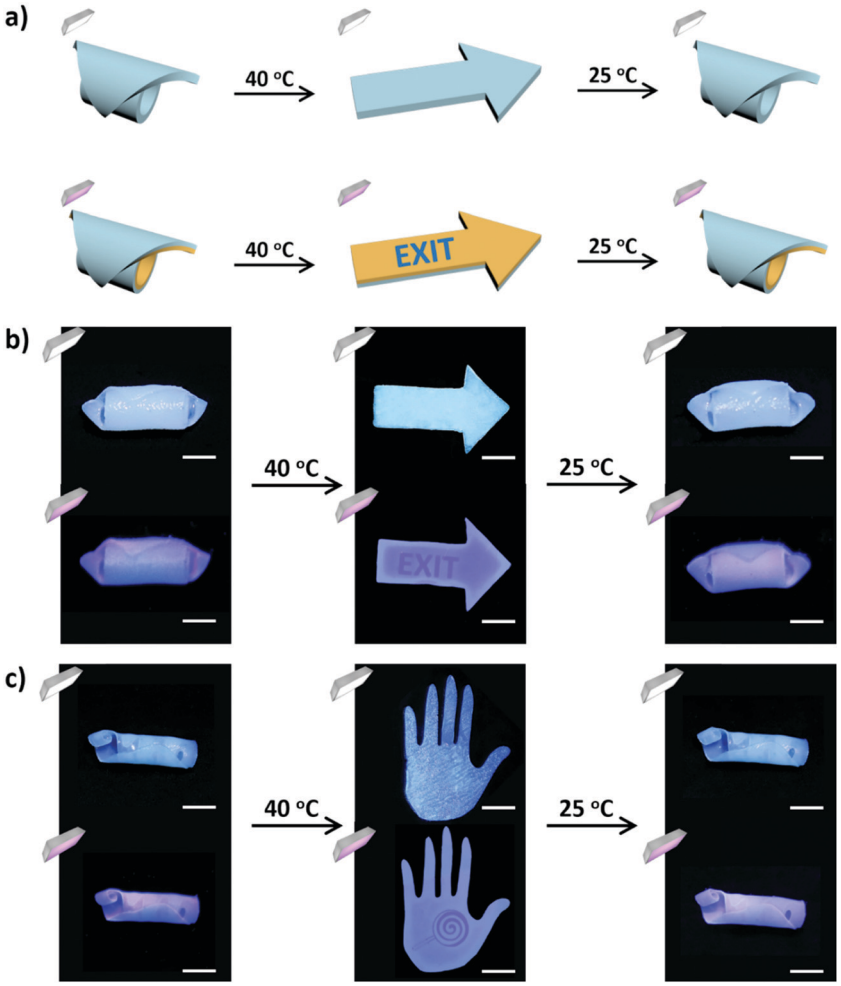

Fig. 5 Encryption and decryption of information in the bilayer hydrogel under specific conditions. (a) Schematic illustration of the decryption process to access the information in the bilayer gel at elevated temperatures and under UV light irradiation from the right direction. (b and c) The fluorescent information of "EXIT" in an arrow-shaped bilayer (b) and a spiral pattern in a hand-shaped bilayer gel (c) becoming readable after being incubated in a 40 °C water bath for shape recovery to the flat shape and under UV light irradiation from the side of the PAV layer. The fluorescent characters and pattern were encoded in the PAV layer of the bilayer gel by photolithography. Scale bar, 5 mm.

the blue fluorescence, and the exposed regions changed to yellow-green fluorescence, creating a blue fluorescent pattern on a yellow-green background. The gel encrypted with patterned fluorescence was transparent and colorless in daylight (Fig. 3d), which was conducive to the concealing of information. We should note that both encoding and reading of fluorescent information are completed under 365 nm UV light, but the light-exposure time for reading was much shorter than that for encoding. Therefore, the fluorescent information could be read at least 20 times. In addition, diverse 2D patterns could be facilely encoded in the PAV layer (Fig. 3e–g), which are stable during the heating–cooling cycles of the bilayer gel.

To further increase the information security of the patterned fluorescence in the PAV layer, UV-absorbing agents were doped in the PAN layer of the bilayer gel to avoid the leakage of information under UV irradiation from the side of the PAN layer. As shown in Fig. S5, ESI,† the bilayer hydrogel was transparent, and the encrypted information of patterned fluorescence could be obviously seen from both sides under UV light. To address this issue, UV-326 was incorporated into the active PAN layer of the bilayer gel. When the bilayer gel was irradiated from the side of the PAN layer, the presence of UV-326 stopped the penetration of UV light to the underneath PAV layer and thus the display of fluorescent information. As shown in Fig. 4a, the PAN gel containing UV-326 showed excellent UV shielding ability when compared to the high transmission of UV light for the gel without UV-326. The different properties are demonstrated in Fig. 4b, where the two PAN gels without and with UV-326 were placed atop two papers written with fluorescent characters by using fluorescein sodium and then irradiated using 365 nm UV light. As expected, the fluorescent characters under the PAN gel without UV-326 were displayed, while the characters under the gel with UV-326 were not. With the protection of the PAN layer with UV-absorbing agents, the fluorescence spectra from the side of the PAN layer of the bilayer hydrogel after UV light irradiation for a long time

exhibited no yellow emission, while the fluorescence spectra from the side of the PAV layer exhibited obvious yellow emission (Fig. 4c). We patterned the word ''EXIT'' in the bilayer gel with UV-326 in the PAN layer by photolithography from the side of the PAV layer. The patterned information was only visible when irradiated from the side of the PAV layer, rather than from the side of the PAN layer (Fig. 4d).

Based on these results, we can realize multi-level encryption of information in the bilayer hydrogel with patterned fluorescence in the passive PAV layer and UV-326 in the active PAN layer (Fig. 5a). The bilayer hydrogel deformed into a roll at room temperature and recovered to the flat shape at an elevated temperature.[49] Multiple conditions are required to decrypt the information concealed in the bilayer hydrogel: heating to flatten the bilayer gel and UV light irradiation from the right direction. This scenario is demonstrated in Fig. 5b and c. At room temperature, the information was not detectable even under the irradiation of UV light due to the roll configuration of the bilayer gel. After being incubated in a 40 °C water bath, the gel became flat to expose the PAV layer. However, the fluorescent information was not visible in daylight. Additional UV light irradiation was imposed to further decrypt the concealed information in the fluorescent form. We should note that the encryption and decryption of information are fully reversible, mediated by various conditions, which is conducive to the delivery of important information with improved security.

Conclusions

In summary, we have described a strategy to improve information security by combining the shape morphing and patterned fluorescence in a bilayer hydrogel that was fabricated by two-step polymerization and a subsequent solvent exchange process. The bilayer gel consisted of an active layer with a UV-absorbing agent to prevent light penetration from this side and a passive layer with tunable fluorescence to enable writing-in patterned information *via* photolithography. At room temperature the bilayer gel deformed into the roll configuration to conceal the information, which cannot be decrypted even under UV light irradiation. The encrypted information was only accessible when a set of conditions were provided: elevated temperature for shape recovery of the bilayer gel to the flat shape and UV light irradiation from the right direction to show the fluorescent information. Although we only showed a simple fluorescent pattern and 3D shapes for multi-encryption of the information, it is feasible to create other information with higher resolution such as the quick-response codes and to obtain more sophisticated configurations of the bilayer gel, considering the advantages of photolithography and the control of morphing structures. This work should open opportunities for gel materials in the field of information encryption and display with high-level security.

Conflicts of interest

There are no conflicts to declare.

Acknowledgements

This work was supported by the National Natural Science Foundation of China (51973189 and 52173012) and the Natural Science Foundation of Zhejiang Province of China (LR19E030002).

References

1 K. Matsushima and N. Sonobe, *Appl. Opt.*, 2018, **57**, A150–A156.
2 X. Guo, J. Zhong, B. Li, S. Qi, Y. Li, P. Li, D. Wen, S. Liu, B. Wei and J. Zhao, *Adv. Mater.*, 2021, **33**, 2103192.
3 H. Sugiyama, T. Sawada, H. Yano and T. Kanai, *J. Mater. Chem. C*, 2013, **1**, 6103–6106.
4 K. Zhong, J. Li, L. Liu, S. Van Cleuvenbergen, K. Song and K. Clays, *Adv. Mater.*, 2018, **30**, 1707246.
5 T. Wu, M. Xie, J. Huang and Y. Yan, *ACS Appl. Mater. Interfaces*, 2020, **12**, 39578–39585.
6 W. Ren, G. Lin, C. Clarke, J. Zhou and D. Jin, *Adv. Mater.*, 2020, **32**, 1901430.
7 Q. Zhu, L. Zhang, K. Van Vliet, A. Miserez and N. Holten-Andersen, *ACS Appl. Mater. Interfaces*, 2018, **10**, 10409–10418.
8 Y. Yao, Y. Wang, Z. Li and H. Li, *Langmuir*, 2015, **31**, 12736–12741.
9 L. Tang, S. Liao and J. Qu, *ACS Appl. Mater. Interfaces*, 2019, **11**, 26346–26354.
10 P. Chen, Q. Li, S. Grindy and N. Holten-Andersen, *J. Am. Chem. Soc.*, 2015, **137**, 11590–11593.
11 C. Y. Li, S. Y. Zheng, C. Du, J. Ling, C. N. Zhu, Y. J. Wang, Z. L. Wu and Q. Zheng, *ACS Appl. Polym. Mater.*, 2019, **2**, 1043–1052.
12 H. Liu, S. Wei, H. Qiu, B. Zhan, Q. Liu, W. Lu, J. Zhang, T. Ngai and T. Chen, *Macromol. Rapid Commun.*, 2020, **41**, 2000123.
13 B. Y. Wu, X. X. Le, Y. K. Jian, W. Lu, Z. Y. Yang, Z. K. Zheng, P. Theato, J. W. Zhang, A. Zhang and T. Chen, *Macromol. Rapid Commun.*, 2019, **40**, 1800648.
14 Y. Xu, J. Chen, H. Zhang, H. Wei, L. Zhou, Z. Wang, Y. Pan, X. Su, A. Zhang and J. Fu, *J. Mater. Chem. C*, 2020, **8**, 247–252.
15 Q. Zhang, Q. Mao, C. Shang, Y.-N. Chen, X. Peng, H. Tan and H. Wang, *J. Mater. Chem. C*, 2017, **5**, 3699–3705.
16 E. A. Widder, *Science*, 2010, **328**, 704–708.
17 M. J. Webber, E. A. Appel, E. W. Meijer and R. Langer, *Nat. Mater.*, 2016, **15**, 13–26.
18 M. McKenzie, D. Betts, A. Suh, K. Bui, L. D. Kim and H. Cho, *Molecules*, 2015, **20**, 20397–20408.
19 S. Mantha, S. Pillai, P. Khayambashi, A. Upadhyay, Y. Zhang, O. Tao, H. M. Pham and S. D. Tran, *Materials*, 2019, **12**, 3323.
20 E. Bat, E. W. Lin, S. Saxer and H. D. Maynard, *Macromol. Rapid Commun.*, 2014, **35**, 1260–1265.
21 Y. Tian, C. Du, B. Liu, H. N. Qiu, X. H. Zhang, Z. L. Wu and Q. Zheng, *J. Polym. Sci.*, 2021, **59**, 904–911.

22 C. N. Zhu, C. Y. Li, H. Wang, W. Hong, F. Huang, Q. Zheng and Z. L. Wu, *Adv. Mater.*, 2021, **33**, 2008057.
23 X. Ji, R. T. Wu, L. Long, X. S. Ke, C. Guo, Y. J. Ghang, V. M. Lynch, F. Huang and J. L. Sessler, *Adv. Mater.*, 2018, **30**, 1705480.
24 T. Oya, T. Enoki, A. Y. Grosberg, S. Masamune, T. Sakiyama, Y. Takeoka, K. Tanaka, G. Wang, Y. Yilmaz, M. S. Feld, R. Dasari and T. Tanaka, *Science*, 1999, **286**, 1543–1545.
25 M. Hua, D. Wu, S. Wu, Y. Ma, Y. Alsaid and X. He, *ACS Appl. Mater. Interfaces*, 2021, **13**, 12689–12697.
26 J. Liao, J. Huang, S. Yang, X. Wang, T. Wang, W. Sun and Z. Tong, *ACS Appl. Polym. Mater.*, 2019, **1**, 2703–2712.
27 Q. Zhao, H. J. Qi and T. Xie, *Prog. Polym. Sci.*, 2015, **49-50**, 79–120.
28 X. L. Gong, Y. Y. Xiao, M. Pan, Y. Kang, B. J. Li and S. Zhang, *ACS Appl. Mater. Interfaces*, 2016, **8**, 27432–27437.
29 Z. J. Wang, W. Hong, Z. L. Wu and Q. Zheng, *Angew. Chem., Int. Ed.*, 2017, **56**, 15974–15978.
30 A. Matsuda and Y. Osada, *Nature*, 1995, **376**, 219.
31 L. Ionov, *Adv. Funct. Mater.*, 2013, **23**, 4555–4570.
32 X. P. Hao, C. Y. Li, C. W. Zhang, M. Du, Z. Ying, Q. Zheng and Z. L. Wu, *Adv. Funct. Mater.*, 2021, **31**, 2000781.
33 Y. Cui, D. Li, C. Gong and C. Chang, *ACS Nano*, 2021, **15**, 13712–13720.
34 X. P. Hao, Z. Xu, C. Y. Li, W. Hong, Q. Zheng and Z. L. Wu, *Adv. Mater.*, 2020, **32**, 2000781.
35 X. Y. Liu, H. Xu, L. Q. Zhang, M. Zhong and X. M. Xie, *ACS Appl. Mater. Interfaces*, 2019, **11**, 42856–42864.
36 Q. L. Zhu, C. F. Dai, D. Wagner, M. Daab, W. Hong, J. Breu, Q. Zheng and Z. L. Wu, *Adv. Mater.*, 2020, **32**, 2005567.
37 J. Ren, X. Shu, Y. Wang, D. Wang, G. Wu, X. Zhang, Q. Jin, J. Liu, Z. L. Wu, Z. Xu, C.-Z. Li and H. Li, *Chin. Chem. Lett.*, 2021, DOI: 10.1016/j.cclet.2021.10.052.
38 H. Kim, J. H. Kang, Y. Zhou, A. S. Kuenstler, Y. Kim, C. Chen, T. Emrick and R. C. Hayward, *Adv. Mater.*, 2019, **31**, 1900932.
39 X. Liu, J. Liu, S. Lin and X. Zhao, *Mater. Today*, 2020, **36**, 102–124.
40 C. N. Zhu, T. Bai, H. Wang, J. Ling, F. Huang, W. Hong, Q. Zheng and Z. L. Wu, *Adv. Mater.*, 2021, **33**, 2102023.
41 Y. Zhang, X. Le, Y. Jian, W. Lu, J. Zhang and T. Chen, *Adv. Funct. Mater.*, 2019, **29**, 1905514.
42 C. N. Zhu, T. Bai, H. Wang, W. Bai, J. Ling, J. Z. Sun, F. Huang, Z. L. Wu and Q. Zheng, *ACS Appl. Mater. Interfaces*, 2018, **10**, 39343–39352.
43 C. Chen, X.-H. Jin, X.-J. Zhou, L.-X. Cai, Y.-J. Zhang and J. Zhang, *J. Mater. Chem. C*, 2015, **3**, 4563–4569.
44 X. H. Jin, C. Chen, C. X. Ren, L. X. Cai and J. Zhang, *Chem. Commun.*, 2014, **50**, 15878–15881.
45 S. I. Druzhinin, V. A. Galievsky and K. A. Zachariasse, *J. Phys. Chem. A*, 2005, **109**, 11213–11223.
46 H. Chen, F. Yang, Q. Chen and J. Zheng, *Adv. Mater.*, 2017, **29**, 1606900.
47 H. Zhang, Q. Li, Y. Yang, X. Ji and J. L. Sessler, *J. Am. Chem. Soc.*, 2021, **143**, 18635–18642.
48 J. Deng, H. Wu, W. Xie, H. Jia, Z. Xia and H. Wang, *ACS Appl. Mater. Interfaces*, 2021, **13**, 39967–39975.
49 S. Y. Zheng, Y. Tian, X. N. Zhang, M. Du, Y. Song, Z. L. Wu and Q. Zheng, *Soft Matter*, 2018, **14**, 5888–5897.

